Journal of Catalysis 269 (2010) 359–366

Contents lists available at ScienceDirect

Journal of Catalysis

journal homepage: www.elsevier.com/locate/jcat

Catalytic conversion of olefins on supported cubic platinum nanoparticles: Selectivity of (1 0 0) versus (1 1 1) surfaces

Ilkeun Lee, Francisco Zaera *

Department of Chemistry, University of California, Riverside, CA 92521, USA

ARTICLE INFO

Article history:
Received 10 September 2009
Revised 18 November 2009
Accepted 19 November 2009
Available online 23 December 2009

Keywords:
Selectivity
Isomerization
Hydrogenation
2-Butene
Platinum
Colloidal synthesis
Kinetics
Surface science
Temperature-programed desorption
Infrared absorption spectroscopy

ABSTRACT

The surface chemistry and catalytic conversion of cis- and trans-2-butenes on platinum (1 0 0) facets were characterized via surface-science and catalytic experiments. Temperature-programed desorption studies on Pt(1 0 0) single crystals pointed to the higher hydrogenation probability of the trans isomer at the expense of a lower extent of C=C double-bond isomerization. To test these trends under catalytic conditions, shape selective catalysts were prepared by dispersing cubic platinum colloidal nanoparticles (which expose only (1 0 0) facets) onto a high-surface-area silica xerogel support. Infrared absorption spectroscopy and transmission electron microscopy were used to determine the conditions needed to remove the organic surfactants without loosing the original narrow size distribution and cubic shape of the original metal nanoparticles. Catalytic kinetic measurements with these materials corroborated the surface-science predictions, and pointed to a switch in isomerization selectivity from preferential cis-to-trans conversion with Pt(1 0 0) surfaces to the reverse trans-to-cis reaction with Pt(1 1 1) facets.

1. Introduction

As catalytic processes become more complex, the issue of selectivity continues to gain more significance. The need for selective catalytic processes arises from the need to minimize the amount of feedstocks consumed, bypass complex purification procedures for the products, and avoid releasing potentially polluting byproducts [1–3]. From a molecular standpoint, selectivity may be achieved by designing specific catalytic sites, perhaps emulating the way enzymes work. Controlling the shape of solid catalysts to produce such specific sites is in general difficult, but recent advances in self-assembly and nanotechnology offer novel approaches toward this goal. The use of catalysts with well-defined shapes has afforded high selectivities in many reactions [3–5].

Particularly promising are new reports on ways to control the shape of metal nanoparticles by using surfactants [6–8]. A multitude of shapes have been achieved by a variety of self-assembly synthetic approaches, including not only simple forms such as nanocubes, nanospheres and nanotetrahedra, but also nanostars, nanorods, nanofibers, nanowires, nanotubes, nanosheets, nanowheels, nanocages, and nanodendrites [9]. Some of these synthetic methodologies have been used in a few instances to prepare supported heterogeneous catalysts [10–13], but an additional challenge needs to be surmounted in such catalysis, the need to disperse the nanoparticles onto a high surface-area support and to pretreat the resulting solid in a way as to remove the organic material used during the nanoparticle synthesis without significantly affecting the shape of the metal clusters [2,8,14,15].

Our group has in recent years focused on the development of selective catalysts for the conversion of hydrocarbons by taking advantage of these new advancements [3,16–22]. Particularly critical to our work has been the identification of the potential effects of surface structure on the selectivity of mild reactions such as hydrogenations and C=C double-bond isomerizations, which have been previously assumed to be structure insensitive [23–26]. In that quest, we have recently shown that the (1 1 1) surfaces of platinum nanocrystals are particularly apt to promote the conversion of trans olefins to their more unstable cis isomers [27–31]. Subsequently, catalysts consisting of platinum tetrahedral nanoparticles, which only expose (1 1 1) facets, were developed and shown to indeed preferentially promote the desirable if thermodynamically unfavorable trans-to-cis conversion [32,33].

In this report we contrast the chemistry of the Pt(1 1 1)-based catalysts to new catalysts based on platinum with (1 0 0) surfaces. Initial surface-science experiments were carried out on Pt(1 0 0) single crystals to test the surface chemistry of cis- and trans-2-butene. Supported catalysts consisting of cubic-Pt nanoparticles were

* Corresponding author. Fax: +1 951 827 3962.
E-mail address: zaera@ucr.edu (F. Zaera).

0021-9517/$ - see front matter © 2009 Elsevier Inc. All rights reserved.
doi:10.1016/j.jcat.2009.11.020

then produced and characterized, and their catalytic behavior toward the conversion of both 2-butenes was tested. Below we summarize the results from these studies, and provide a brief discussion on the contrasting catalytic behavior of cubic-versus tetrahedral-Pt nanoparticles.

2. Materials and methods

Temperature-programed desorption (TPD) experiments were carried out in an ultrahigh vacuum (UHV) system described in detail previously [34,35]. Briefly, a UTI 100C quadrupole mass spectrometer was employed for these experiments, retrofitted with a retractable nose cone terminated in a 5-mm-in-diameter aperture that can be placed within 1 mm of the surface of interest for the selective detection of molecules desorbing from the front face of the crystal. The mass spectrometer is interfaced to a personal computer capable of monitoring the time evolution of up to 15 different masses in a single TPD run. A constant heating rate, 10 K/s in the experiments reported here, is set by homemade electronics. The Pt(1 0 0) single crystal, a polished disk ~1 cm in diameter and ~1 mm in thickness, was mounted on a long-travel manipulator capable of cooling down to ~90 K and resistively heating to 1100 K, and its temperature measured by a chromel–alumel thermocouple spot-welded to its side. The surface was routinely cleaned by cycles of oxidation and annealing in vacuum, and occasionally by Ar^+ sputtering. Gas exposures were performed by backfilling of the vacuum chamber, and are reported in Langmuirs (1 Langmuir = 10^{-6} Torr s), not corrected for differences in ion-gauge sensitivities. All gas dosing was done at temperatures below 100 K.

The cubic platinum nanoparticles were prepared by a procedure also reported in detail before [32] where an aqueous solution of K_2PtCl_4 and sodium polyacrylate (SPA, average MW ~ 2100 amu) was reduced with hydrogen gas and let to rest until the growth of the nanoparticles was evident. The silica xerogel support was synthesized in-house by combining 30% aqueous ammonia and ammonium fluoride solutions with a 1:2 vol:vol ethanol:water mixture, stirring the resulting liquid into a separate ethanol solution of tetraethylorthosilicate (TEOS), and evaporating the solvent at 325 K until a white powder was obtained [36]. The silica xerogel powder was calcined to 675 K before use. To prepare the supported catalyst, the silica xerogel was added to a water-based colloidal solution of the cubic-Pt nanoparticles, and the mixture was sonicated and filtrated. The resulting wet powder was dried and calcined in air and oxidized and reduced three times in a quartz tube under flowing O_2 and H_2, respectively, all at the temperatures indicated in each specific case.

Characterization of the catalysts during the different stages of calcination and oxidation–reduction were carried out by transmission infrared (IR) absorption spectroscopy, using a cell for in situ spectra recording during gas exposures [37,38]. Additional characterization was performed by transmission electron microscopy (TEM), using a Philips TECNAI 12 instrument [39]. The kinetics of conversion of both cis- and trans-2-butenes with hydrogen were measured in a 150-ml close-loop recirculation reactor that can be evacuated with a mechanical pump to a base pressure of approximately 5×10^{-2} Torr, as measured by a thermocouple gauge and a capacitance manometer [40–42]. Samples (5 mg) of the catalysts were placed in a U-shaped quartz tube, a part of the reactor loop, and held in place by quartz wool plugs. Heating of the U tube was done with an Omega furnace equipped with an Omron temperature controller. The reactants (hydrogen, 2-butene, and argon) were introduced sequentially into the loop to the desired partial pressures (0.2, 10, and 590 Torr, respectively), and were mixed using a recirculation bellows pump. Aliquots (10-ml) of the gas sample were taken at 20-min intervals during the catalytic reactions and were analyzed by gas chromatography (GC) using a 23% SP-1700 on 80/100 Chromosorb PAW column (30 ft × 1/8 in. o.d., stainless steel; Supelco) and a flame ionization detector.

The cis-2-butene (>95% purity), trans-2-butene, (>95% purity), and deuterium (>99.5% atom purity) were all purchased from Matheson, and the hydrogen (>99.995% purity) and argon (99.998% purity) were obtained from Liquid Carbonic. Al gases were used as received.

3. Results

3.1. Temperature-programed desorption (TPD) on Pt(1 0 0)

The thermal chemistry of cis- and trans-2-butene on Pt(1 0 0) single-crystal surfaces was first characterized by TPD experiments under ultrahigh vacuum (UHV) conditions. The relevant results for the two isomers are reported in Figs. 1 and 2, respectively. Data from three sets of experiments are shown, carried out on clean (top traces) and hydrogen- (second traces from the top) and deuterium- (remaining traces) predosed surfaces. Desorption is reported for the butenes (left panels) and butanes (right) that are produced in these reactions. In the case of deuterium preadsorption, a maximum olefin isotope exchange of only two deuteriums was seen, presumably because of the preferential reactivity of the inner carbon atoms [27,28].

On clean Pt(1 0 0), only molecular 2-butene desorption was detected. However, the kinetics of that desorption appears to be somewhat complex, and results in the appearance of three TPD peaks with cis-2-butene, at 250, 265, and 310 K, and two with the trans isomer, at 252 and 282 K. Multiple TPD features with hydrocarbons is not unusual, in part because it is possible for the adsorbates to rearrange to different adsorption geometries as the surface coverage changes during temperature ramping [43]. Regardless, the total yield for cis-2-butene is larger than that for

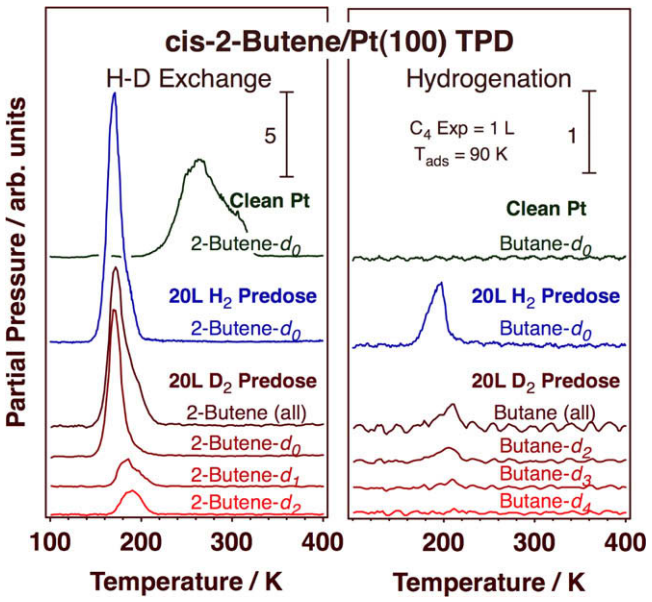

Fig. 1. Temperature-programed desorption (TPD) traces for 1.0 L of cis-2-butene adsorbed on a Pt(1 0 0) single-crystal surface under ultrahigh vacuum (UHV) conditions. Data are provided for the desorption of the relevant H–D exchange (left panel) and hydrogenation/deuteration (right) products. The results are reported from TPD experiments with cis-2-butene adsorbed on a clean surface (top traces), and on surfaces predosed with 20 L of either H_2 (second from top) or D_2 (remaining traces). Several observations are worth highlighting, including the significant lowering of the temperature of the cis-2-butene molecular desorption upon hydrogen/deuterium preadsorption, and the production of butanes and butenes with multiple deuterium substitutions.

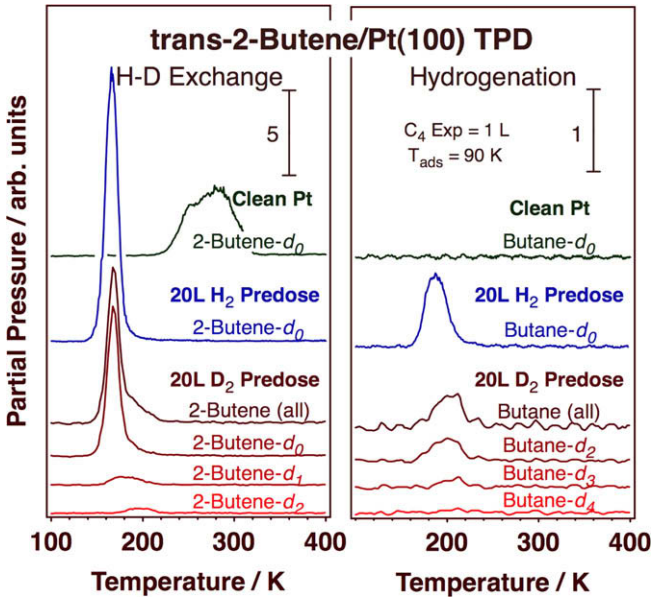

Fig. 2. TPD traces for 1.0 L of trans-2-butene adsorbed on a Pt(1 0 0) single-crystal surface under UHV conditions. As in Fig. 1, data are provided for the desorption of the relevant H–D exchange (left panel) and hydrogenation/deuteration (right) products, and for experiments on clean (top traces) and H_2 (second from top) and D_2 (remaining traces) predosed surfaces. A few differences are seen in comparison with the results obtained from experiments using the cis isomer (Fig. 1), including an increase in hydrogenation yield (which also happens at lower temperatures) at the expense of the formation of isotopically exchanged butenes.

trans-2-butene, in particular in the low-temperature region of the desorption, suggesting that the latter adsorbs more strongly on clean Pt(1 0 0) than the former.

Presaturation of the Pt(1 0 0) surface with either hydrogen or deuterium leads to a large shift of the molecular desorption peak toward lower temperatures. The resulting, much sharper, TPD features now peak at 170 and 167 K with the cis and trans isomers, respectively. The cis reactant appears to be slightly more stable than the trans butene, and both significantly more weakly bound than on the clean surface. All this is consistent with what has been seen on Pt(1 1 1), both with butenes [28] and with other olefins [34], and signifies a switch from di-σ to π adsorption upon hydrogen coadsorption [44–46]. The switch in relative stability between the cis and trans isomers was also observed on Pt(1 1 1) [28], and reproduced by DFT calculations [30].

When coadsorbed with deuterium, it appears that cis-2-butene undergoes more extensive isotope scrambling than the trans isomer. Indeed, larger TPD peaks are seen with the former olefin. However, the feature obtained for 2-butene-d_1 with the trans isomer peaks at a lower temperature: 180 K, versus 187 K with the cis-2-butene reactant. A similar trend on Pt(1 1 1) was previously explained in terms of a higher relative stability of the cis isomer [30] and by a more favorable trans-to-cis conversion than the reverse cis-to-trans reaction (each H–D exchange is accompanied by a cis–trans interconversion) [27,28]. However, the picture is complicated in the Pt(1 0 0) case by competition with hydrogenation (deuteration) steps, a problem not encountered in the studies on Pt(1 1 1). To notice in particular is the early desorption of butane-d_2 with trans-2-butene, which starts around 160 K and peaks at 200 K. By contrast, no 2-butane-d_2 is produced with cis-2-butene until 170 K, and that peaks at 207 K. Also, the onset for 2-butene-d_1 production starts at almost 10 K lower temperatures with trans-2-butene than with cis-2-butene. Further exchange is seen in both cases as well: 2-butene-d_2 desorption peaks at 190 and 198 K with cis- and tran-2-butene, respectively, and butane-d_3 at 210 and 212 K. All these observations lead us to conclude that on Pt(1 0 0) H–D exchange is, in absolute terms, easier with trans-2-butene, that is, the reaction rate constant for H–D exchange with trans-2-butene is larger than that for cis-2-butene. However, the overall isomerization yield is reduced for the case of trans-2-butene because of competition with a more favorable hydrogenation pathway. This is the reason why, overall, a cis-to-trans isomerization preference is observed with the supported catalyst (see below).

3.2. Preparation and characterization of cubic-Pt nanoparticle-based catalysts

In order to test the selectivity of Pt(1 0 0) surfaces in catalysis, supported catalysts using platinum nanocubes were prepared by following the colloidal synthesis described in Section 2. Cubic-Pt nanoparticles expose (1 0 0) planes exclusively, and should therefore reproduce the chemistry seen in the TPD experiments. Since the bigger challenge in this research is the need to device a procedure for eliminating the organic matter bonded to the nanoparticles (the surfactant) after dispersion on the silica support and for activating the catalysts without a significant loss of nanoparticle shape (or size), the effect of calcination and oxidation–reduction treatments under different conditions was followed by infrared absorption spectroscopy. A summary of the relevant data is reported in Fig. 3.

The left panel of Fig. 3 provides reference spectra for sodium polyacrylate (SPA, the surfactant used to make the Pt nanocubes), silica, and the SPA–Pt nanoparticles, each alone and in different combinations in both solid and aqueous phases. Regardless of the surroundings, both SPA and silica display distinct identifying IR absorption bands, at 1402, 1456, and 1558 cm^{-1} for the former and at ~1630 cm^{-1} for the latter. The data also show that, as expected, the IR spectra from the freshly prepared cubic-Pt/SiO_2 catalysts display all four features (middle trace in left panel, top trace in center panel, and bottom trace in right panel). On the other hand, the spectra shown in the center panel of Fig. 3 clearly indicate that either calcination of the catalyst at 775 K or treatment with three cycles of oxidation and reduction at 625 K leads to the elimination of the surfactant; only the peak at 1630 cm^{-1}, the one due to silica, remains after such treatments. The right panel of Fig. 3, which displays IR traces after calcination at different temperatures, indicates that the surfactant is burned at temperatures somewhere between 575 and 675 K.

The nature of the supported catalysts obtained after calcination at different temperatures can be evaluated more directly by observation of the TEM images reported in Fig. 4. In general, those pictures show good dispersion, and also excellent homogeneity in terms of the size and shape of the Pt nanoparticles. No significant changes in those properties occur upon calcination at temperatures of up to 575 K. The results from a statistical analysis of TEM images such as these are provided in Fig. 5. In terms of size, the nanoparticles display a narrow distribution of sizes, with an edge dimension averaging 5.0 ± 0.2 nm (95% confidence) and approximately 60% of the nanoparticles in a bracket between 4.5 and 5.5 nm. Regarding shape, almost 90% of the original colloidal nanoparticles have cubic shape, but some do loose their form upon deposition onto the silica; only approximately 60% survive this process (about 10% adopt a more spherical shape). A slight further shape loss is seen after calcination at temperatures above 525 K, at which point close to 10% of the cubic nanoparticles adopt a rounder structure.

3.3. Kinetics of the catalytic conversion of 2-butenes on cubic-Pt/SiO_2 catalysts

The selectivity of the nanocube-Pt catalysts toward the conversion of olefins was tested in a small batch reactor by using cis- and

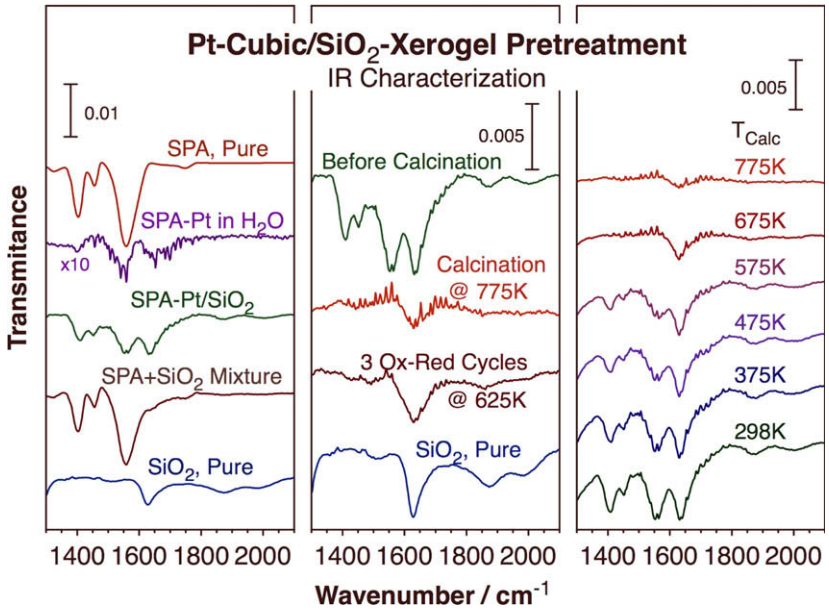

Fig. 3. Transmission infrared (IR) absorption spectra from cubic platinum nanoparticles dispersed on a silica xerogel high-surface-area support after different stages of treatment to remove the surfactant used to prepare the Pt colloidal nanoparticles. The left panel offers reference spectra to help identify the origin of the different IR absorption bands. The center panel highlights the elimination of the signals from the organic surfactants upon either calcination at 775 K or repeated cycles of oxidation in O_2 and reduction with H_2 at 625 K. The right panel provides evidence for the complete removal of the organic matter after calcination at temperatures above 575 K.

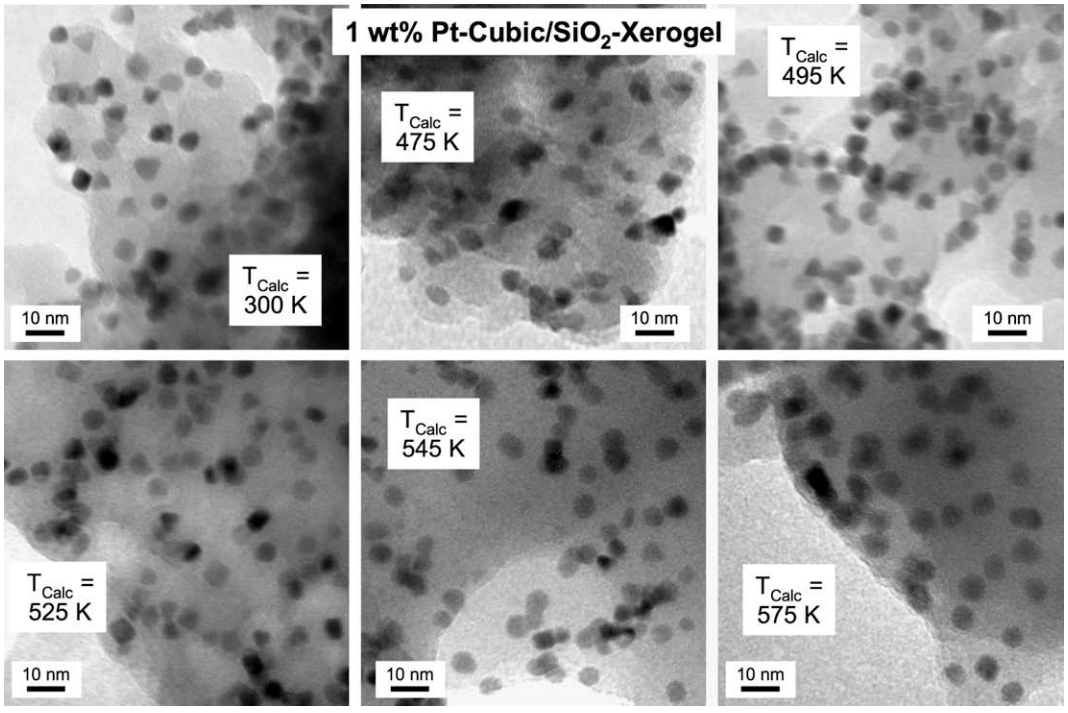

Fig. 4. Transmission electron microscopy (TEM) images of catalysts comprised of cubic platinum nanoparticles dispersed on a silica xerogel after calcination at different temperatures up to 575 K. Almost no changes in either size or shape are apparent from these pictures.

trans-2-butenes as probe molecules. A high hydrocarbon-to-hydrogen ratio, 10 Torr:0.2 Torr, was used in order to favor isomerization over hydrogenation reactions. The accumulation of all main products, 1-butene, cis-2-butene, trans-2-butene, and butane, was followed as a function of reaction time by gas chromatography. Typical raw data in the form of partial pressures versus time are shown in Fig. 6 for cis-2-butene and a catalyst calcined and reduced at 475 K. Initial rates were estimated from the slopes of product accumulation at $t = 0$ s, and were converted to turnover frequencies (TOFs, in molecules per platinum atom per second) by assuming all Pt nanoparticles to be 5-nm-edge-size nanocubes lying flat on the silica support (with 5 the 6 facets exposed).

Evident from the data shown in Fig. 6 is the fact that the rate of conversion for 2-butene + hydrogen mixtures reaches a maximum at temperatures about 425 K. All reactions are activated, and therefore accelerate with increasing temperatures, but by 475 K sufficient carbonaceous deposits accumulate on the surface to partially poison the catalyst [18,47,48]. Poisoning of the catalyst

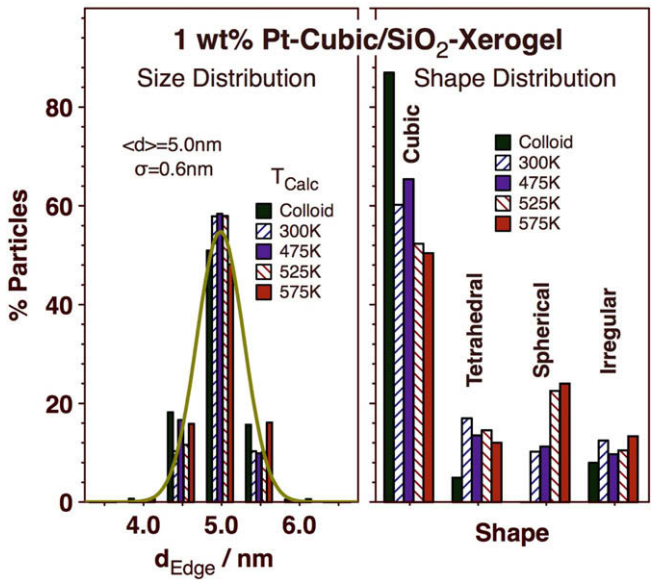

Fig. 5. Statistical analysis of the size and shape of the supported cubic-Pt nanocatalysts derived from TEM pictures such as those shown in Fig. 4. Narrow size distributions with an average nanoparticle size of 5.0 nm were obtained in all cases irrespective of the calcination temperature used. In terms of shape, only approximately 60% of the nanoparticles supported on the silica are cubic, but most of those retained their shape upon calcination to temperatures of up to 575 K; only a small conversion of approximately 10% of the nanoparticles to more spherical shapes was observed about 525 K.

is also manifested by a decrease in reaction rates over time, although that is in part a consequence of the consumption of the hydrogen in the mixture; both hydrogenation and C=C isomerization reactions typically display positive orders in hydrogen partial pressure [49,50], and the small amount of H_2 used in these experiments means that P_{H_2} changes significantly even after the small conversions shown in Fig. 6. Regardless, measurable conversions were observed in these experiments for the first 200 s of reaction. Also, C=C isomerizations to 1-butene and trans-2-butene (to 1-butene and cis-2-butene when starting with trans-2-butene) proved to be faster under the chosen conditions than the hydrogenation to butane.

The initial rates obtained with both cis- (left panel) and trans- (right) 2-butene at 425 K are reported in Fig. 7 as a function of the temperature used for calcination and reduction of the catalyst prior to use. Significant decreases in rate were seen with calcination temperature, a trend that we do not fully understand at the present time, in particular because it is not as marked at other reaction temperatures. Regardless, similar hydrogenation rates were measured with both isomers, but faster isomerization rates were always observed with the cis isomer. It does appear that the higher thermodynamic stability of trans-2-butene may affect the overall rate of its conversion. Two more observations are worth highlighting from this figure: (1) the selectivity for 1-butene production is always higher than that for cis–trans interconversion; and (2) the selectivity for cis-2-butene conversion to trans-2-butene is higher than that for trans-to-cis conversion when starting with trans-2-butene.

Finally, selectivity in the conversion of both olefins is reported in Fig. 8 for three reaction temperatures on cubic and on tetrahedral platinum nanoparticles. The data shown here represent an average over results obtained using catalysts treated at several calcination temperatures, the whole range used in our experiments with the cubic nanoparticles and those for calcinations up to 525 K in the tetrahedral-Pt case. These temperature ranges were selected to cover the conditions where nanoparticle shape is preserved (as established by TEM after reaction [32]) and no large selectivity changes are observed. Key conclusions from this figure include: (1) with both cubic and tetrahedral nanoparticles, and with both cis- and trans-2-butenes, higher reaction temperatures result in higher selectivities for 1-butene formation and less hydrogenation to butane; (2) selectivity for cis–trans interconversion also goes down with temperature, albeit to a lesser extent (the effect is less noticeable with the tetrahedral nanoparticles); (3) hydrogenation to butane is always more favorable with trans-2-butene than with the cis isomer; (4) at all reaction temperatures, cis-to-trans isomerization is more favorable than trans-to-cis

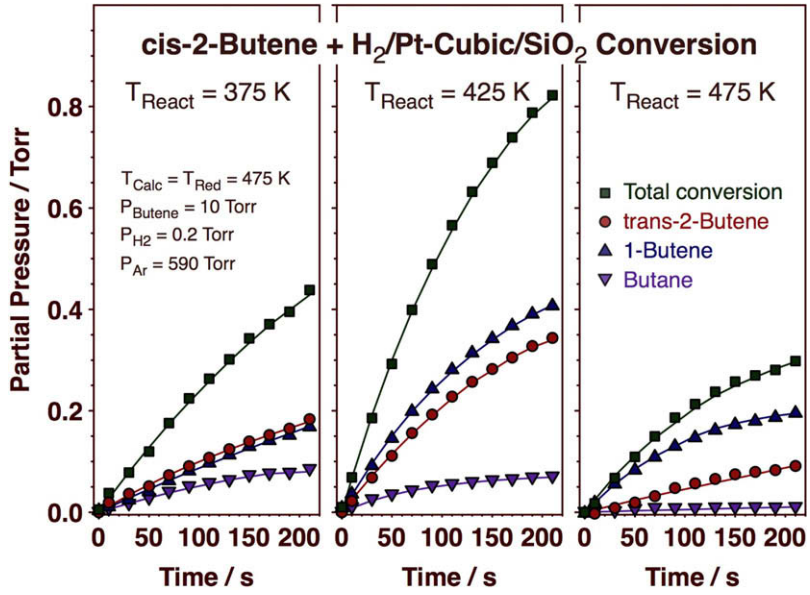

Fig. 6. Kinetic data for the conversion of cis-2-butene with hydrogen on a supported cubic-Pt nanoparticles catalyst at three different reaction temperatures. In this figure, the accumulations in the batch reactor of the relevant products (trans-2-butene, 1-butene, and butane) are shown as a function of reaction time. Optimal activity was seen around 425 K; lower temperatures resulted in lower rates because the reactions are activated, and higher temperatures led to poisoning of the catalyst via the deposition of carbonaceous deposits.

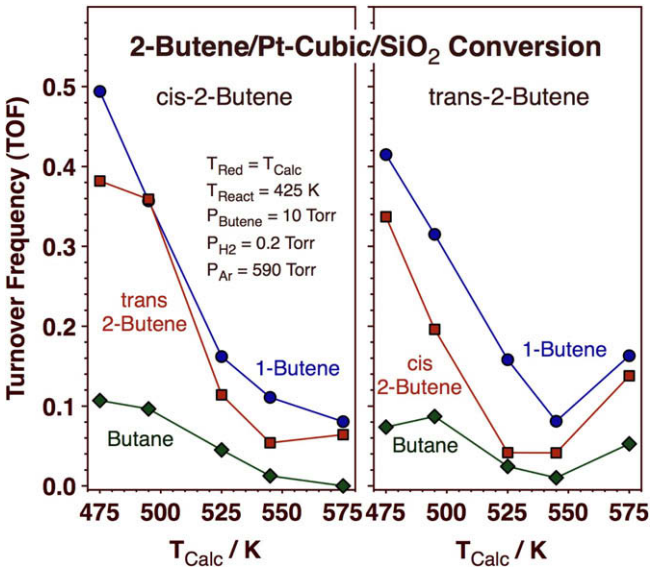

Fig. 7. Initial reaction rates for the conversion of cis- (left panel) and trans- (right) 2-butene on the cubic-Pt/silica catalyst as a function of calcination temperature. A reduction in total activity is seen with increasing calcination temperature, and a higher activity is observed with the cis isomer.

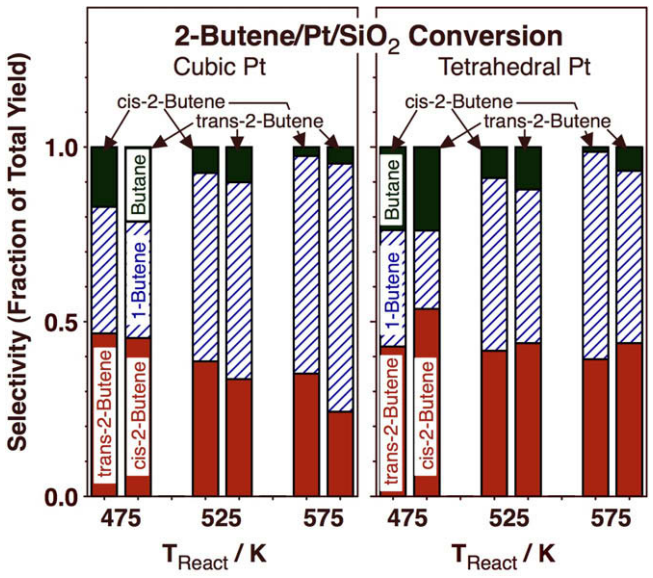

Fig. 8. Selectivities for the conversion of cis- (left columns in each pair) and trans- (right columns) 2-butenes on dispersed cubic (left panel) and tetrahedral (right) platinum nanoparticles as a function of reaction temperature. Several differences are seen between the performance of the two types of catalysts, significantly a switch in the preference for cis–trans isomerization but also a higher hydrogenation selectivity with the tetrahedral catalysts.

conversion on cubic-Pt catalysts, while with tetrahedral nanoparticles the reverse is the case; (5) selectivity for cis-to-trans conversion always increases relative to trans-to-cis with reaction temperature; and (6) cubic-Pt catalysts promote more isomerization to 1-butene and less hydrogenation to butane (in relative terms) than tetrahedral-Pt samples.

4. Discussion

In this report, data are provided for the thermal conversion of cis- and trans-2-butene on Pt(1 0 0) surfaces. Results from temperature-programed desorption (TPD) experiments on single crystals under vacuum and from catalytic studies using cubic-Pt nanoparticles dispersed on a high-surface-area silica support are contrasted for the two reactants. Comparisons with similar experiments reported previously on Pt(1 1 1) surfaces are also included. The general purpose of this work was to expand our initial studies on the control of reaction selectivities for C=C double-bond isomerization reactions via control of the shape of supported platinum catalysts [32,33]. Mild reactions such as this have been traditionally considered structure insensitive [51,52], but it is our contention that this is only because there has not been sufficient control over the nature of the catalysts [3]. The novel self-assembly synthetic techniques developed recently by the nanomaterials community [6–8] have now afforded a new approach to gain exquisite control on the size and shape of metal nanoparticles and to test our hypothesis.

An initial insight on the potential differences in the thermal chemistry of olefins on different facets of metal surfaces comes from surface-science experiments using single crystals. In general, the Pt(1 0 0) surfaces appear to be more active for olefin isomerization and olefin hydrogenation than the Pt(1 1 1) counterparts, since all butene desorption in the TPD experiments reported in Figs. 1 and 2 peaks below 200 K (on the hydrogen-presaturated surfaces). This contrasts with the broader and higher-temperature TPD features reported previously for Pt(1 1 1) [27,28,33], and also for the stepped Pt(5 5 7) and rougher Pt(1 1 0)–(2 × 1) surfaces [33]. However, the higher reactivity of the Pt(1 0 0) crystal does not appear to transfer to the shape-controlled supported catalysts: the cubic-Pt nanoparticles displayed, in general, activities approximately 2–3 times lower than the tetrahedral-Pt nanoparticles in terms of conversion per gram of catalyst. This is partly compensated by the fact that the tetrahedral nanoparticles have a larger percentage of their atoms exposed (approximately 50% versus 30% for the cubic nanoparticles), but that alone is not sufficient to explain the whole difference in activity measured in the kinetic work. Several reasons can be cited for the remaining discrepancy, including possible differences in the efficiency with which the organic matter is removed from the catalyst during pretreatment, and also differences in the percentage of low-coordination atoms in tetrahedral versus cubic nanoparticles.

Another key difference between the chemistry of the 2-butenes on Pt(1 0 0) versus Pt(1 1 1) single crystals seen by TPD is the fact that only in the former significant hydrogenation to butane is observed; only butenes and hydrogen desorb from the Pt(1 1 1) surface [28]. This complicates the kinetic picture for the Pt(1 0 0) facets, because the hydrogenation reaction competes with C=C double-bond isomerization steps, and, consequently, affects the final yields for cis- versus trans-2-butene formation. Specifically, the temperatures seen for the desorption of butene-d_1, which reflects a single cis–trans interconversion, indicate a higher absolute rate for trans-to-cis isomerization relative to the cis-to-trans reaction, the same as on Pt(1 1 1). However, hydrogenation (or deuteration) is also faster with trans-2-butene, to the point of favorably competing with the isomerization step. Overall, the yield for cis-2-butene obtained in TPD experiments from trans-2-butene is significantly smaller than the yield of trans-2-butene from the isomerization of cis-2-butene. This is most likely the reason why cubic-Pt nanoparticles appear to preferentially promote the conversion of the cis isomer to its trans counterpart in the catalytic experiments.

Most of the other conclusions derived from the TPD experiments are also reflected in the results obtained with the Pt nanoparticle catalysts. For instance, higher hydrogenation selectivities were also observed with the trans isomer of 2-butene. On the other hand, the catalytic data introduce one additional factor to consider, the isomerization of the 2-butenes to 1-butene. This is a reaction difficult to follow in TPD, because the mass spectra of all three

butene isomers are quite similar (which is the reason why H–D exchange was used as proxy for the cis–trans interconversion) [27]. Significant amounts of 1-butene are always produced with the supported Pt catalysts, more in relative terms with the nanocubes than with the tetrahedral nanoparticles. Also, the selectivity toward 1-butene formation was always seen to increase with temperature, an indication that the activation energy for that reaction is higher than those for 2-butene cis–trans interconversion and hydrogenation. The latter observation is consistent with past surface-science reports, and is explained by a lower probability for beta-hydride elimination from the terminal methyl groups of the 2-butyl surface intermediate common to all three reactions [3,53,54]. The former conclusion suggests that the reaction probabilities differences may be less marked on Pt(1 0 0), that is, that beta-hydride elimination may be less selective on that surface.

We end with a brief discussion of the ability to prepare supported catalysts with well-defined metal nanoparticles, not only in terms of size but also with respect to shape. These new catalysts should open new possibilities in the field of catalysis in terms of selectivity control [2,33]. Indeed, the ideas in terms of differences in relative rates among competing pathways in the conversion of 2-butenes on (1 1 1) versus (1 0 0) facets of platinum may be quite general, extending to other reactions, other metals, and other crystallographic orientations of the surface. Critical to this approach is the ability to prepare and activate supported catalysts based on colloidal metal nanoparticles without loosing the narrow distributions in size and shape obtained after their initial synthesis. We [32,33] and others [2,8,14,15] have shown that it is not always easy to remove the organic matter used for the preparation of the nanoparticles once those are dispersed onto high-surface-area supports without affecting their structural properties. It is also important to evaluate the possible changes that may occur on the nature of the nanoparticles during the course of the reaction. This is particularly important in demanding and highly exothermic reactions [55], but is less of an issue with mild reactions such as the hydrogenation and C=C double-bond isomerizations discussed here. Certainly, no significant changes in catalyst shape were seen after reactions with 2-butene using supported tetrahedral-Pt nanoparticles [32].

An interesting observation from our work is the higher stability of supported cubic-Pt nanoparticles relative to that of tetrahedral-Pt nanoparticles. It is noted that virtually no changes were seen here upon treating the dispersed cubic nanoparticles to temperatures up to 575 K. With the tetrahedral nanoparticles, significant loss in shape was reported at that temperature, by which point the fraction of tetrahedral nanoparticles was reduced from almost 80% to approximately 20% [33]. This is at first somewhat surprising, because (1 1 1) surfaces, those exposed by tetrahedral nanoparticles, are more stable than (1 0 0) facets, the ones seen with cubic nanoparticles. However, it should be acknowledged that in small nanoparticles a significant percentage of atoms are in low-coordination sites such as edges and corners. In fact, even though the tetrahedral and cubic nanoparticles synthesized in our work had similar edge dimensions, approximately 5.0 nm in both cases, that corresponds to much smaller tetrahedral nanoparticles in terms of their volume, with only ~20% of the total number of Pt atoms per nanoparticle of the cubic nanostructures. Consequently, there are almost twice as many low-coordination atoms in the tetrahedral versus cubic nanoparticles. There may be a stronger driving force with tetrahedral-Pt nanoparticles to reconstruct to minimize the high surface tension implied by such high fraction of unstable atoms. Another factor to consider is the relative stability of the organic capping agent used in making the colloidal nanoparticles, which were different for the cubic and tetrahedral nanoparticles (SPA versus PVP) [32]. The end result, according to our IR studies (Fig. 3), is that, while all the PVP can be calcined from the supported tetrahedral nanoparticles by 575 K, higher temperatures are required to remove the SVA from the cubic nanoparticles. This could justify the higher shape stability of the latter, and also their lower catalytic activity.

5. Conclusions

The reactivity of Pt(1 0 0) surfaces toward the conversion of 2-butenes was evaluated both in surface-science studies under vacuum and by catalytic studies using cubic nanoparticles dispersed on porous silica. The results from temperature-programed desorption experiments with Pt(1 0 0) single crystals indicate significantly higher overall reactivity than on Pt(1 1 1). Also, detectable hydrogenation to butane is possible on hydrogen-presaturated (1 0 0) surfaces but not on (1 1 1) facets. On deuterium-predosed surfaces, H–D exchange is observed as well, an indication of cis–trans interconversion. More hydrogenation (deuteration) and less H–D exchange are seen with trans-2-butene relative to cis-2-butene. The rate constant for trans-to-cis conversion is still larger than that for the equivalent cis-to-trans reaction, as on Pt(1 1 1); the lower H–D exchange yields seen in the first case are due to losses to the hydrogenation pathway.

Catalysts with high fractions of Pt(1 0 0) facets were prepared via the synthesis of cubic-Pt nanoparticles using colloidal methodology and their dispersion onto a high-surface-area silica xerogel support. Activation of the resulting catalysts to remove the organic surfactant was characterized in some detail by infrared absorption spectroscopy and electron microscopy. Calcination temperatures above 575 K are required to eliminate the organic material, more stringent conditions than those needed to treat equivalent catalysts made out of tetrahedral-Pt nanoparticles. On the other hand, the cubic nanoparticles proved to be more stable, maintaining their size and shape even after calcination at 575 K. Well-defined catalysts were prepared this way, with average sizes of 5.0 ± 0.2 nm, and more than half of the supported nanoparticles having cubic shape.

The catalytic conversion of both cis- and trans-2-butene in the presence of small amounts of hydrogen was tested with the cubic-Pt nanoparticle catalyst. Optimum reactivity was seen around 425 K, a temperature high enough to promote the activated reactions yet low enough to minimize the buildup of irreversibly adsorbed carbonaceous deposits. Due to the low partial pressures of hydrogen used, C=C double-bond isomerizations dominated over hydrogenation to butane, which never amounted to more than 20% of the total products. Higher reaction temperatures led to more relative 1-butene production, which was in all cases higher than with tetrahedral-Pt. In terms of cis–trans isomerization around the C=C double-bond, cis-to-trans conversion was always faster with cubic Pt than the reverse trans-to-cis reaction. This is the opposite of the behavior previously reported with tetrahedral Pt, a fact that highlights the structure sensitivity of the isomerization reaction.

Acknowledgment

Financial support for this project was provided by a Grant from the US National Science Foundation.

References

[1] F. Zaera, J. Phys. Chem. B 106 (2002) 4043.
[2] G. Somorjai, C. Kliewer, React. Kinet. Catal. Lett. 96 (2009) 191.
[3] F. Zaera, Acc. Chem. Res. 42 (2009) 1152.
[4] R. Narayanan, M.A. El-Sayed, J. Phys. Chem. B 109 (2005) 12663.
[5] G.A. Somorjai, J.Y. Park, Angew. Chem., Int. Ed. 47 (2008) 9212.
[6] C. Burda, X. Chen, R. Narayanan, M.A. El-Sayed, Chem. Rev. 105 (2005) 1025.
[7] E. Ramirez, L. EradÉs, K. Philippot, P. Lecante, B. Chaudret, Adv. Funct. Mater. 17 (2007) 2219.
[8] A.R. Tao, S. Habas, P. Yang, Small 4 (2008) 310.

[9] L. Wang, Y. Yamauchi, Chem. Mater. 21 (2009) 3562.
[10] J.W. Yoo, D. Hathcock, M.A. El-Sayed, J. Phys. Chem. A 106 (2002) 2049.
[11] Z. Konya, V.F. Puntes, I. Kiricsi, J. Zhu, P. Alivisatos, G.A. Somorjai, Catal. Lett. 81 (2002) 137.
[12] A. Miyazaki, I. Balint, Y. Nakano, J. Nanopart. Res. 5 (2003) 69.
[13] J.C. Serrano-Ruiz, A. López-Cudero, J. Solla-Gullón, A. Sepúlveda-Escribano, A. Aldaz, F. Rodríguez-Reinoso, J. Catal. 253 (2008) 159.
[14] H. Lee, S.E. Habas, S. Kweskin, D. Butcher, G.A. Somorjai, P. Yang, Angew. Chem., Int. Ed. 45 (2006) 7824.
[15] C. Wang, H. Daimon, T. Onodera, T. Koda, S. Sun, Angew. Chem., Int. Ed. 47 (2008) 3588.
[16] F. Zaera, Appl. Catal. A 229 (2002) 75.
[17] F. Zaera, Catal. Today 81 (2002) 149.
[18] F. Zaera, Catal. Lett. 91 (2003) 1.
[19] F. Zaera, J. Phys.: Condens. Mat. 16 (2004) S2299.
[20] F. Zaera, Top. Catal. 34 (2005) 129.
[21] F. Zaera, J. Mol. Catal. A 228 (2005) 21.
[22] F. Zaera, Chem. Rec. 5 (2005) 133.
[23] B. Brandt, J.-H. Fischer, W. Ludwig, S. Schauermann, J. Libuda, F. Zaera, H.-J. Freund, J. Phys. Chem. C 112 (2008) 11408.
[24] B. Brandt, W. Ludwig, J.H. Fischer, J. Libuda, F. Zaera, S. Schauermann, J. Catal. 265 (2009) 191.
[25] R. Morales, F. Zaera, J. Phys. Chem. B 110 (2006) 9650.
[26] R. Morales, F. Zaera, J. Phys. Chem. C 111 (2007) 18367.
[27] I. Lee, F. Zaera, J. Am. Chem. Soc. 127 (2005) 12174.
[28] I. Lee, F. Zaera, J. Phys. Chem. B 109 (2005) 2745.
[29] I. Lee, F. Zaera, J. Phys. Chem. C 111 (2007) 10062.
[30] F. Delbecq, F. Zaera, J. Am. Chem. Soc. 130 (2008) 14924.
[31] I. Lee, M.K. Nguyen, T.H. Morton, F. Zaera, J. Phys. Chem. C 112 (2008) 14117.
[32] I. Lee, R. Morales, M.A. Albiter, F. Zaera, Proc. Natl. Acad. Sci. USA 105 (2008) 15241.
[33] I. Lee, F. Delbecq, R. Morales, M.A. Albiter, F. Zaera, Nat. Mater. 8 (2009) 132.
[34] F. Zaera, D. Chrysostomou, Surf. Sci. 457 (2000) 89.
[35] I. Lee, Z. Ma, S. Kaneko, F. Zaera, J. Am. Chem. Soc. 130 (2008) 14597.
[36] <http://eetd.lbl.gov/ecs/aerogels/sa-making.html>.
[37] F. Zaera, Int. Rev. Phys. Chem. 21 (2002) 433.
[38] H. Tiznado, S. Fuentes, F. Zaera, Langmuir 20 (2004) 10490.
[39] <http://micron.ucr.edu/>.
[40] A. Loaiza, M. Xu, F. Zaera, J. Catal. 159 (1996) 127.
[41] M. Aryafar, F. Zaera, Catal. Lett. 48 (1997) 173.
[42] J. Wilson, H. Guo, R. Morales, E. Podgornov, I. Lee, F. Zaera, Phys. Chem. Chem. Phys. 9 (2007) 3830.
[43] F. Zaera, Acc. Chem. Res. 35 (2002) 129.
[44] F. Zaera, Langmuir 12 (1996) 88.
[45] H. Öfner, F. Zaera, J. Phys. Chem. 101 (1997) 396.
[46] H. Öfner, F. Zaera, J. Am. Chem. Soc. 124 (2002) 10982.
[47] S.M. Davis, F. Zaera, G.A. Somorjai, J. Catal. 77 (1982) 439.
[48] Z. Ma, F. Zaera, Surf. Sci. Rep. 61 (2006) 229.
[49] G.C. Bond, Metal-Catalysed Reactions of Hydrocarbons, Springer, New York, 2005.
[50] F. Zaera, G.A. Somorjai, J. Am. Chem. Soc. 106 (1984) 2288.
[51] F.M. Dautzenberg, J.C. Platteeuw, J. Catal. 24 (1972) 364.
[52] B.C. Gates, J.R. Katzer, G.C.A. Schuit, Chemistry of Catalytic Processes, McGraw-Hill, New York, 1979.
[53] S. Tjandra, F. Zaera, J. Am. Chem. Soc. 117 (1995) 9749.
[54] C.J. Jenks, B.E. Bent, F. Zaera, J. Phys. Chem. B 104 (2000) 3017.
[55] S.J. Kweskin, R.M. Rioux, S.E. Habas, K. Komvopoulos, P. Yang, G.A. Somorjai, J. Phys. Chem. B 110 (2006) 15920.